Experimental Thermal and Fluid Science 83 (2017) 231–238

Contents lists available at ScienceDirect

Experimental Thermal and Fluid Science

journal homepage: www.elsevier.com/locate/etfs

# Experimental investigation on incipient mass flow rate of micro aluminum powder at high pressure

Haijun Sun, Chunbo Hu *, Xiaofei Zhu, Jiangang Yang

*School of Astronautics, Northwestern Polytechnical University, Xi'an 710072, China*

ARTICLE INFO

*Article history:*
Received 30 July 2016
Received in revised form 9 January 2017
Accepted 14 January 2017
Available online 17 January 2017

*Keywords:*
Semi-empirical model
Powder entrainment
Incipient mass flow rate
Powder engine
High pressure

ABSTRACT

Experiments on powder entrainment have been carried out to study the influence of different variable parameters on incipient mass flow rate. A semi-empirical model was established by taking into account many affecting parameters, including: initial total pressure, particle mean size, throttling orifice area and powder volume fraction. This model could be used to predict the incipient mass flow rate with particle mean sizes from 10 μm to 100 μm. By comparing the relative error between the semi-empirical model and previous model, the results show that the semi-empirical model has higher prediction accuracy than previous model.

In the progress of particle entrainment, there exists three stages: flow-out stage with gas (stage I), flow-out stage with large amounts of particles (stage II), and flow-out stage with small amount of particles (stage III). The result of stage I shows that there exists a pickup delay for particles, which is good for the ignition sequence matching research of powder engine.

© 2017 Elsevier Inc. All rights reserved.

## 1. Introduction

Since using metal powder as fuel, and gas or solid particles as oxidant, powder engine has the functions of thrust regulation and multiple pulse ignition. In the early 1960s, American Bell Aerospace Company first launched the ignition validation work for aluminum powder (AL)/ammonium perchlorate (AP) powder rocket engine [1–3]. However, this project was rarely reported because it was put on hold due to limitation of powder fluidization and particle combustion technologies. As the fields of deep space detection and hypersonic flight vehicle springing up gradually, the powder engine concept has been put forward, such as Mg/CO2 powder rocket engine used for Mars exploration and the metal powder scramjet engine used for hypersonic flight vehicle [4–9]. Other work like experimental verification on them has also been widely carried out [10–13].

In the developing process of powder engine, the high efficiency technology for particle ignition is one of the key research points, and successful engine ignition is not only depends on the powder fuel's own physical and chemical properties, but also the state of powder fluidization and conveying.

At present, there are many public research reports on ignition properties of particle fuel (such as magnesium, aluminum, and boron), and some ignition mechanisms of particles were revealed, which are beneficial to the design of engine ignition energy to a certain extent [14,15]. However, previous ignition mechanism researches were mainly based on static particles. It is not applicable to powder engine for its requirement of particle dynamic ignition. As a result, it is necessary to study the ignition characteristics of powder fuel in moving state.

As one of major influence factors for powder engine ignition, the value of incipient powder mass flow rate directly relates to the success of ignition. When working conditions remain the same for ignition energy, excessive incipient mass flow rate of powder may lead to ignition failure because of deficiency for existing ignition energy, and the overlarge mass flow rate may blow off the initial flame even successful ignition. However, if the incipient powder mass flow rate is too small, the instable and small flame will form in the early stage, which may finally lead to ignition failure too. So the entrainment characteristics of particles need to be studied first due to the incipient powder mass flow rate is mainly affected by that.

Particle entrainment characteristic is an important parameter in particle-liquid systems, such as movement of sand dunes, slurry conveying, dispersion of particles in liquids and gas-solid conveying in industry applications. Although the previous researches of particle entrainment characteristics mainly focus on the pickup

* Corresponding author.
*E-mail address:* huchunbo@nwpu.edu.cn (C. Hu).

http://dx.doi.org/10.1016/j.expthermflusci.2017.01.012
0894-1777/© 2017 Elsevier Inc. All rights reserved.

**Nomenclature**

| | |
|---|---|
| $\dot{m}$ | powder mass flow rate (kg/s) |
| $\dot{m}_{\text{model}}$ | is powder mass flow rate calculated by model (kg/s) |
| $\dot{m}_{\text{exp.}}$ | is powder mass flow rate measured by experiment. (kg/s) |
| $m_{packing}$ | actual packing mass of powder (kg) |
| $V_{box}$ | total volume of powder chamber ($m^3$) |
| $A$ | cross-sectional area of throttling orifice ($m^2$) |
| $C_P$ | effective heat capacity of particles (J/mol·K) |
| $C_{P,g}$ | the constant pressure heat capacity of gas (J/mol·K) |
| $R_g$ | gas constant (J/mol·K) |
| $R_m$ | gas-solid two-phase constant |
| $T$ | stagnation temperature (K) |
| $P_0$ | stagnation pressure (Pa) |
| $P$ | initial total pressure (Pa) |
| $d_P$ | particle diameter (m) |
| $Re_p$ | particle Reynolds number |
| $Ar$ | Archimedes number |
| $U_{pu}$ | particle pick up velocity (m/s) |
| $g$ | gravity acceleration ($m/s^2$) |
| $g_0$ | radial distribution function |

*Greek letters*

| | |
|---|---|
| $\rho_p$ | particle density ($kg/m^3$) |
| $\rho$ | gas density ($kg/m^3$) |
| $\gamma_g$ | gas adiabatic index |
| $\gamma_m$ | gas-solid adiabatic index |
| $\phi$ | particle mass fraction |
| $\varepsilon_p$ | particle volume fraction |
| $\mu$ | gas viscosity (Pa·s) |
| $\tau_p$ | particle relaxation time (s) |
| $\tau_l$ | collision time interval of particles (s) |
| $\theta$ | granular temperature ($m^2/s^2$) |

velocity and mechanism [16–19], instead of paying attention to the entrainment rate directly, that can also provide a good idea for incipient mass flow rate research.

In this paper, we investigated the incipient powder mass flow rate of powder engine under different influencing factors, and built one prediction model of entrainment rate based on the particle pick up mechanism, which lays a solid experimental foundation for the research on ignition properties of powder engine.

## 2. Experimental

In our previous work [20], we found there would be a mass flow rate peak at high pressure, as is shown in Fig. 1. The particle pickup process with rather instable powder mass flow rate is so short, and the value of mass flow rate is different to that in steady stage, thus it is necessary to study the initial process specially. An experimental system has been designed to measure the powder mass flow rate in initial stage, as is shown in Fig. 2.

The experimental system is mainly composed of gas cylinder, powder chamber, pneumatic ball valve, control computer and powder collector. Where the pneumatic ball valve is used as a switch of powder conveying, with a response time of 50 ms. The minimum cross-sectional area of conveying pipeline is controlled by throttle orifice. In order to prevent dust dispersion, the cyclone separator is used to collect powder. At the beginning of experiment, put the pre-weighted powder into powder chamber, after that fill fluidized gas into it to a certain pressure, and then stop gas supply. Afterwards, open the pneumatic ball valve, the high-pressure gas in powder chamber will carry the powder through throttling orifice to the powder collector. After shutting down the pneumatic ball valve, there will some residual gas in the powder chamber, which needs to be discharged through pipe with sleeve filter in it to exclude the effect of fluidized gas weight.

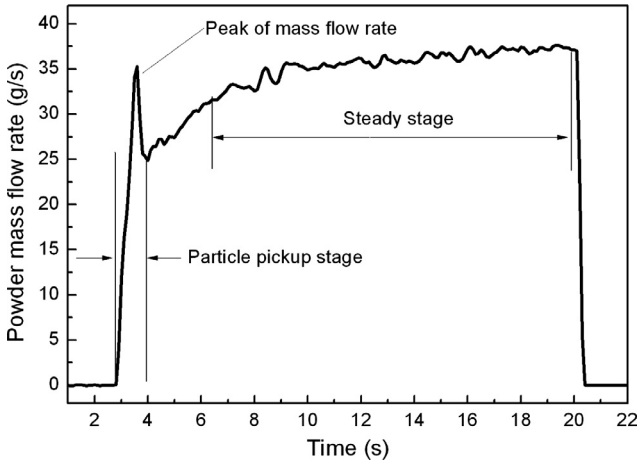


**Fig. 1.** The peak of powder mass flow rate.

The process of powder mass flow rate peak is relatively short, about one second in Fig. 1. For convenience of analysis, set the time interval equal to one second as powder entrainment time, which means during the experiment, the pneumatic ball valve should be shut down immediately when working one second later. Considering the response time of pneumatic ball valve exists in both opening stage and closing stage, the time interval of one second would largely unaffected by response time. Thus, the mass of spouting powder through throttling orifice is called as the incipient mass flow rate. By calculating the mass difference of powder in chamber before and after the experiment, the powder entrainment rate can be determined. The working medium is fine aluminum powder for that is a common fuel in powder engine, and the fluidized gas is inert nitrogen.

The experimental operating conditions are shown in Table 1, there lists four main influence factors, including initial total pressure, throttling orifice diameter, particle diameter and powder volume fraction. Where the mean particle diameter is refers to the volume weighted mean diameter, and the typical size distribution of particle is shown in Fig. 3. The formula of powder volume fraction $\varepsilon_P$ in Table 1 is as follows:

$$\varepsilon_p = \frac{m_{packing}}{V_{box}\rho_p} \times 100\% \tag{1}$$

where $m_{packing}$ is the actual packing mass of powder, $V_{box}$ is the total volume of powder chamber; $\rho_p$ is the density of aluminum particle.

## 3. Previous model

According to the principle of gas choking, the gas solid two-phase flow was assumed to equilibrium flow, and there would be a gas solid "choking" phenomenon for equilibrium flow. Based on gas solid equilibrium flow, Wang et al. deduced the formula of particle mass flow rate [21]:

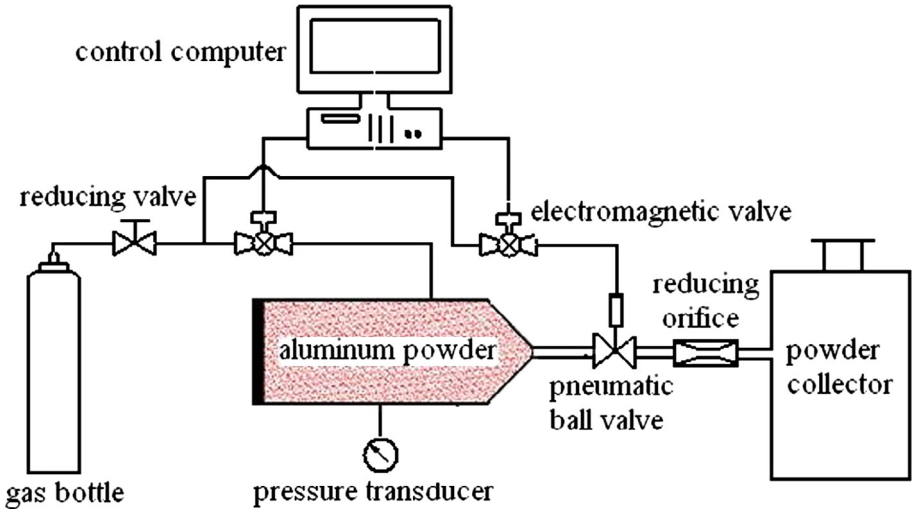


**Fig. 2.** Experimental system.

**Table 1**
Experimental conditions.

| Main influencing factors | Rang |
|---|---|
| Initial total pressure (MPa) | 0.5–5 |
| Diameter of throttling orifice (mm) | 1.5–3 |
| Mean particle diameter (μm) | 20–80 |
| Volume fraction of powder (%) | 38–55 |

$$\dot{m} = \frac{P_0 A}{\sqrt{R_m T}} \sqrt{\gamma_m} \left[\frac{2}{\gamma_m + 1}\right]^{\frac{\gamma_m + 1}{2(\gamma_m - 1)}} \tag{2}$$

$$\gamma_m = \gamma_g \left(1 + \frac{\phi}{1-\phi} \frac{C_P}{C_{P,g}}\right) \Big/ \left(1 + \frac{\phi}{1-\phi} \frac{C_P}{C_{P,g}} \gamma_g\right) \tag{3}$$

$$R_m = R_g(1-\phi)/(1-\varepsilon_p) \tag{4}$$

where $\dot{m}$ is powder mass flow rate, $P_0$ is stagnation pressure, $A$ represents cross-sectional area of throttling orifice, $R_m$ is two-phase mixture constant, $R_g$ is gas constant, $T$ represents stagnation temperature, $\gamma_m$ represents gas-solid adiabatic index, $\gamma_g$ represents gas adiabatic index, $\phi$ represents particle mass fraction, $C_P$ represents effective heat capacity of particles, $C_{P,g}$ represents the constant pressure heat capacity of gas, $\varepsilon_p$ is particle volume fraction.

Seen from the formulas above, the major factors are stagnation pressure, cross-sectional area of shrink nozzle, powder mass fraction and volume fraction, etc., which can give some physical meanings of gas-solid flow for powder mass flow rate. On the other hand, the items of solid material properties like particle diameter and density are not included in formula (2), so the calculated results of gas-solid mass flow rate will be the same when changing particle diameter or density only, which does not meet the gas-solid flow laws. Even in some special conditions, when particle diameter is bigger than shrink nozzle diameter, the particle mass flow rate will be zero in fact, so there would be a physical error for formula (2).

## 4. Results and discussions

In the Cabrejos and Klitzing's research of particle pickup velocity, the Reynolds number and Froude number were presented to describe the pickup mechanism of particle [22], which makes the experimental results to be more meaningful. However, Kalman et al. [17] found that the pickup mechanism would be described better by using Reynolds and Archimedes numbers. The representations of three dimensionless quantities are as follows:

$$\text{Reynolds number} = \frac{\text{inertial force}}{\text{viscous force}};$$

$$\text{Froude number} = \frac{\text{inertial force}}{\text{gravity force}}$$

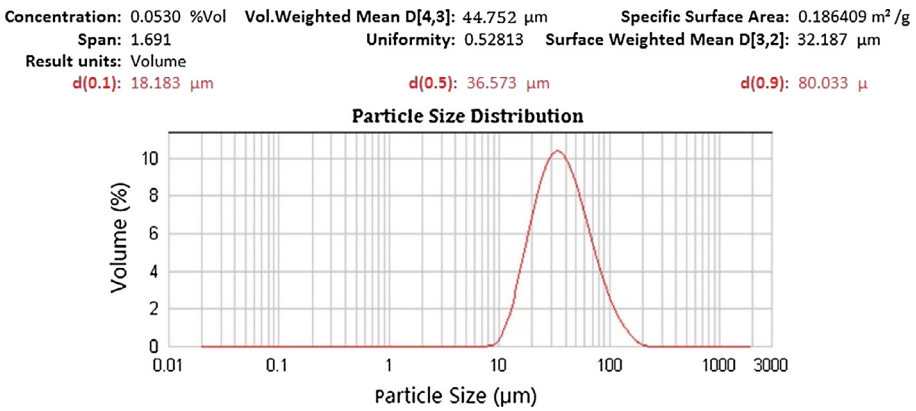


**Fig. 3.** Particle size distribution.

$$\text{Archimedes number} = \frac{\text{inertial force} \times \text{buoyancy force}}{(\text{viscous force})^2}$$

From above, we know that the Archimedes number covers buoyancy force and viscous force instead of gravity force, because the buoyancy and viscous forces are affected by particle diameter, particle density and fluid density directly, and there exists a quite agreement of experimental results for Reynolds number as a function of Archimedes number [17]. Thus, Reynolds and Archimedes numbers can describe the pickup mechanism in a more comprehensive way than Reynolds and Froude numbers, and it is also benefit for the analysis of particle pick up at high pressure. Where the Reynolds number $Re_p$ and Archimedes number $Ar$ are defined as:

$$Re_p = \frac{\rho U_{pu} d_p}{\mu} \tag{5}$$

$$Ar = \frac{g\rho(\rho_p - \rho)d_p^3}{\mu^2} \tag{6}$$

where $\rho$ is gas density, $\rho_p$ is particle density, $U_{pu}$ is particle pick up velocity, $d_P$ is particle diameter, $\mu$ is gas viscosity, g is gravity acceleration.

In Ref. [16–17,23], they found there would be a relationship between Reynolds number and Archimedes number by analyzing the experiments results, and the function is as follows:

$$Re_p = aAr^b \tag{7}$$

where $a$ and $b$ are the coefficients, which are determined by experimental results.

Actually, the particle pick up velocity is refers to the fluid velocity required to initiate sliding, rolling, suspension and blowing away of particle at rest [17,24]. The bigger fluid velocity required, the more difficult for particle to be picked up, and the powder entrainment will be less, there exists an inverse relationship phenomenon between particle entrainment rate and pick up velocity from experimental results. Not only that, but from Eq. (2) we know particle mass flow rate is also inversely proportional to $\sqrt{R_m T}$, where $\sqrt{R_m T}$ is refers to the velocity of gas-solid mixture. Thus it can be seen from Refs. [17,24] and Eq. (2) that the particle pick up velocity can be used to represent the particle entrainment rate, as follows:

$$\dot{m} \propto \frac{1}{U_{pu}} \tag{8}$$

With reference to the form of Eq. (2), we built an approximate relationship for particle entrainment rate based on Eq. (8), as Eq. (9) shows:

$$\dot{m} = f(\varepsilon_p)\frac{PA}{U_{pu}} \tag{9}$$

where $P$ is initial total pressure, and that is proportional to gas density according to the ideal gas law (10), $A$ is throttling orifice area, $f(\varepsilon_p)$ is the coefficient and was defined as the function of particle volume fraction for easy analysis. It's because that the parameters such as mixture density, mixture constant and specific heat ratio are all directly related to particle volume fraction, and particle mass fraction is also directly related to particle volume fraction too, so the function of particle volume fraction can be used to represent the coefficients of above variables.

$$P = \rho R_g T \tag{10}$$

Substituting Eqs. (5) and (10) into expression (9), as follows:

$$\dot{m} = f(\varepsilon_p)\frac{(\rho R_g T)A\rho d_p}{Re_p \mu} \tag{11}$$

Seen from above Eq. (11), there is no particle density item, so particle mass flow rate will be the same by changing particle density only, which does not follow the physical law. Therefore, we added the particle density item to Eq. (11) by replacing one fluid density item, and the influence of item changing will be represented by $f(\varepsilon_p)$ finally, which is determined by experimental results. Substituting Eqs. (6) and (7) into Eq. (11) to form the final model of particle incipient mass flow rate, as follows:

$$\dot{m} = f(\varepsilon_p)\frac{(\rho R_g T)A\rho_p d_p}{a\mu[g\rho(\rho_p - \rho)d_p^3/\mu^2]^b)} \tag{12}$$

### 4.1. Effects of pressure and particle diameter

Fig. 4 shows a relationship between particle incipient mass flow rate and initial total pressure. As can be seen, incipient mass flow rate increases with total pressure, and the law is qualitatively consistent with the formula (2), where the particle mass flow rate has a linear relationship with the stagnation pressure, but in Fig. 4, the mass flow rate changes in logarithm relation instead of direct proportion to the total pressure.

In Fig. 4, the relationship between incipient mass flow rate and particle size (10–100 μm) is nonlinear. Instead, the incipient mass flow rate increases first and decreases later as the particle size increases. So there would be a maximum value for incipient mass flow rate when the particle size is appropriate, this is because the dominant forces are different when particle with different sizes.

Dasani et al. [17,18] studied the particle pickup velocity in horizontal tube and found the pickup velocity is mainly depends on the particle sizes. When particle at large diameters (>50 μm), gravity force plays a leading role and particle pickuped individually. At small particle diameters (<20 μm), the cohesion forces, such as electrostatic and van der Waals forces, become much more significant. At intermediate particle size ranges (20–50 μm); the cohesive forces (van der Waals) are considerable but still the particles are picked up individually, so gravity force and cohesive force play a mutual effect. Thus it can be seen that if the particle diameter is 20 μm, the particles will be pickuped agglomerates instead of individually due to the cohesive forces are big enough and play a main role, which leading to flow prevention for particles. When particle diameter is 75 μm, gravity force plays a main role, so gas drag needs to overcome the gravity force to pickup the particles, which makes the particle with small incipient mass flow rate. However, if

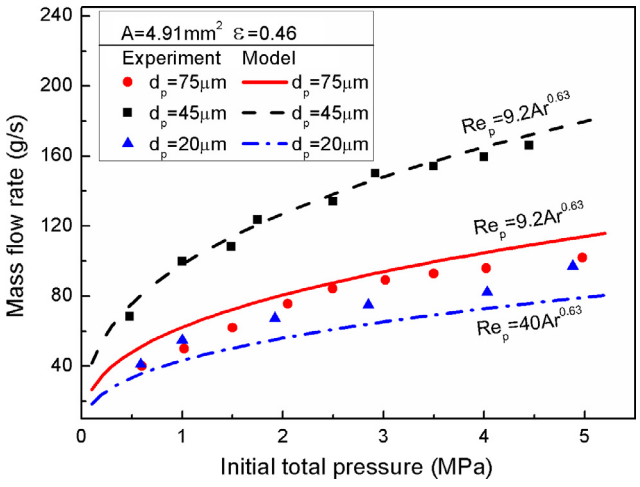


**Fig. 4.** Relationship between incipient mass flow rate and initial total pressure with different particle diameters.

the particle diameter is 45 μm, at an intermediate particle size, the cohesive force coordinates with gravity force. When both of them achieve a relatively balanced state, the particles would easily flow out under the effect of gas phase, thus the incipient mass flow rate is the largest.

The correlation coefficients of formula (12) can be determined by experimental data fitting, where $f(\varepsilon) = 4.627 \times 10^{-4}$ for particle volume fraction is a constant. The Reynolds number and Archimedes number under different particle sizes are shown as below:

$$Re_p = 40Ar^{0.63} \quad \text{for} \quad d_p = 20\ \mu\text{m} \tag{13}$$

$$Re_p = 9.2Ar^{0.63} \quad \text{for} \quad d_p = 45\ \mu\text{m and } d_p = 75\ \mu\text{m} \tag{14}$$

On the other hand, the model results shown in Fig. 4 agree well with the experiments, which indicate that the current incipient mass flow rate model is reasonable.

### 4.2. Effect of throttle orifice area

From the formulas (2) and (12), we know that the incipient mass flow rate is in proportion to throttling orifice area, and the comparisons of model and experiment are shown in Figs. 5and 6. With different particle sizes, the incipient mass flow rate increases with the throttling orifice area, and the model values coincide better with the measured results, which shows that it is appropriate for model (12) by using first power of throttling orifice area to represent the influence of gas solid exit.

Initial total pressure and throttling orifice area are the two big influence factors on particle mass flow rate, the incidence of which can be represented by the slope of incipient mass flow rate. From the m (12) we know the incipient mass flow rate is in relation to initial total pressure and throttling orifice area, as follows:

$$\dot{m} \propto \frac{P}{[P(c-P)]^b} \tag{15}$$

$$\dot{m} \propto A \tag{16}$$

where c and b are coefficients. Do a single differential for the above formulas, the change rate of initial total pressure and throttling orifice area can be obtained.

$$\frac{d\dot{m}}{dP} = \frac{(2b-1)}{P^{b-1}(P-a)^{b+1}} + \frac{c(c-b)}{P^b(P-a)^{b+1}} \tag{17}$$

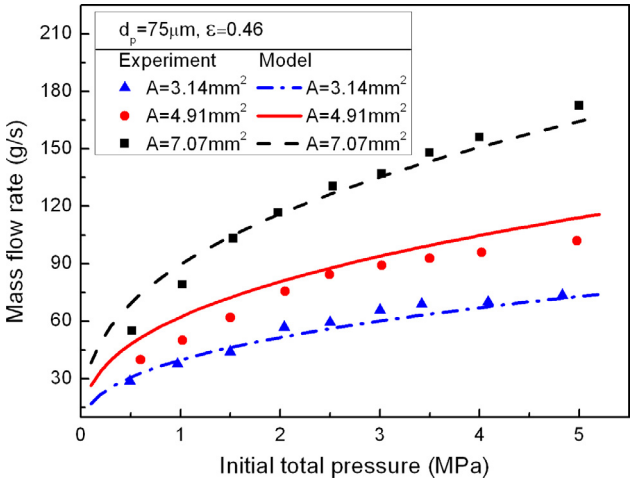


**Fig. 5.** Relationship between incipient mass flow rate and throttle orifice area with particle diameter is 75 μm.

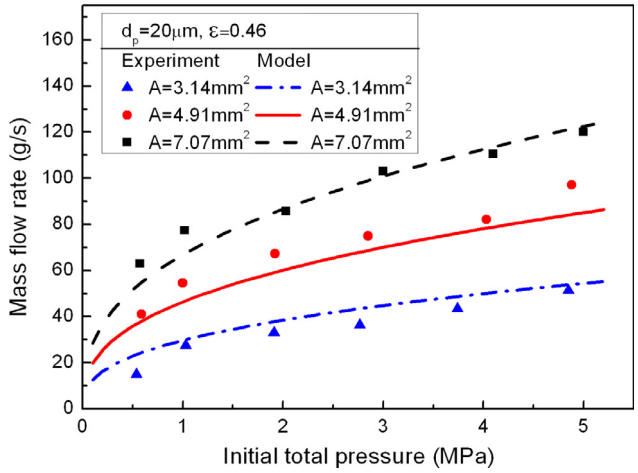


**Fig. 6.** Relationship between incipient mass flow rate and throttle orifice area with particle diameter is 20 μm.

$$\frac{d\dot{m}}{dA} = constant \tag{18}$$

The increasing rate of incipient mass flow rate decreases with the increase of initial total pressure, but it is a constant when increase the throttling orifice area, which indicates there would be an obvious change for incipient mass flow rate by adjusting throttling orifice area.

### 4.3. Effect of powder volume fraction

Powder volume fraction mainly influences the specific heat ratio of gas solid mixture and has a great effect on incipient mass flow rate. The relationship between incipient mass flow rate and volume fraction under the condition of different throttling orifice area is shown in Fig. 7. As is shown, the incipient mass flow rate shows an s-shaped increase law as the powder volume fraction increases, and no matter the powder volume fraction is relatively small or big, the increasing amplitude of incipient mass flow rate is relatively small, while in appropriate volume fraction range, the increasing amplitude turns to big obviously.

To same extent, both of the relaxation time and collision time interval of particles are affected by particle volume fraction, where the relaxation time is defined as the time-taken for static particle accelerates to the 63% of fluid velocity, which shows the following

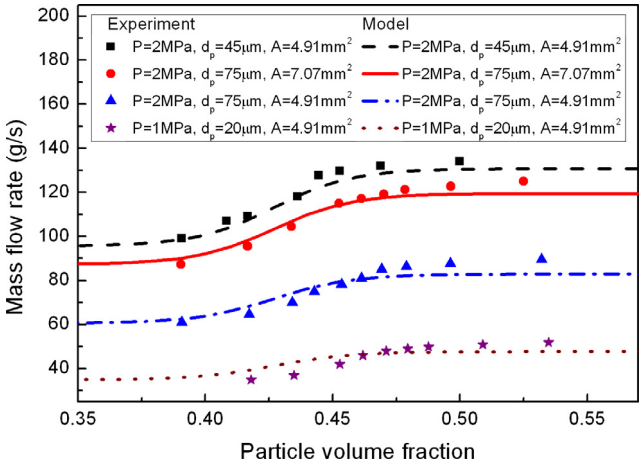


**Fig. 7.** Relationship between incipient mass flow rate and powder volume fraction.

feature of particle. The relaxation time $\tau_p$ and collision time interval $\tau_l$ are defined as follows [25]:

$$\tau_p = \frac{\rho_p d_p^2 (1-\varepsilon_p)^{3.65}}{18\mu(1-0.15Re_p^{0.687})} \tag{19}$$

$$\tau_l = \frac{d_p}{24\varepsilon_p g_0}\left(\frac{\pi}{\theta}\right)^{0.5} \tag{20}$$

where $g_0$ is radial distribution function, $\theta$ is granular temperature.

The formula (19) shows that the relaxation time decreases with the increase of particle volume fraction, particles can be easily picked up for its following feature enhancement, that is benefit for incipient mass flow rate augment. Otherwise, the collision time interval between particles also decreases as volume fraction increases, the shorter collision time interval, the higher collision frequency, so the kinetic energy loss of particles would be caused by high collision frequency, which results in a decrease of particle pick up energy. On the other hand, the high collision frequency leads to a high contact probability for particles, which enlarges the viscous force and decreases the pickup kinetic energy too. Thus it can be seen that the incipient mass flow rate increases with particle volume fraction, but the increasing range decreases when the particle volume fraction increases to a certain extent, and the particle collision has a great effect on the increasing range of incipient mass flow rate.

In formula (12), the function of particle volume fraction is used to represent the parameter coefficients, because there is a s-shaped increase law between incipient mass flow rate and volume fraction increases, the function $f(\varepsilon_p)$ needs to be a s-shaped curve too. The expression of $f(\varepsilon_p)$ is obtained by experimental datas fitting, as follows:

$$f(\varepsilon_p) = 4.7608\times10^{-4} - \frac{1.28008\times10^{-4}}{1+e^{(\varepsilon_p-0.42713)/0.01531}} \tag{21}$$

The final semi-empirical model of particle incipient mass flow rate is:

$$\dot{m} = \left(4.7608\times10^{-4} - \frac{1.28008\times10^{-4}}{1+e^{(\varepsilon_p-0.42713)/0.01531}}\right)\frac{(\rho R_g T)A\rho_p d_p}{a\mu[g\rho(\rho_p-\rho)d^3/\mu^2]^b} \tag{22}$$

where $\begin{cases} a=40, b=0.63 \text{ for } d_p=20\ \mu m \\ a=9.2, b=0.63 \text{ for } d_p=45\ \mu m \text{ and } 75\ \mu m \end{cases}$.

The comparison of model datas and experimental results is shown in Fig. 6, the model datas agree well with the experimental datas except some conditions of small particle diameter (20 μm) and throttling orifice area (3.14 $mm^2$). It is because some parameter coefficients are represented by formula (22) totally, which leads to a fuzzy processing for some parameter coefficients that greatly influence on some conditions.

It is worth noting that when powder volume fraction reaches to a certain value, the increasing amplitude of incipient mass flow rate with the increase of volume fraction is not obvious. This law provides an engineering reference for the determination of incipient mass flow rate in powder engine. Larger fuel density specific impulse can greatly improve the powder engine performance, so it requires a high powder volume fraction. When powder volume fraction reaches to a certain value, the incipient mass flow rate is virtually determined, that is called critical mass flow rate. Thus, the larger incipient mass flow rate can be amended on the basis of critical mass flow rate which is corresponding to a critical volume fraction.

### 4.4. Error analysis

Since the semi-empirical model (22) is based on limited experimental data with a narrow range of variable-value, the applicability of this model has a certain limitations. So the model datas were compared with the corresponding test datas under the same working condition to test the accuracy of prediction model, and the relative error was put forward to represent the model accuracy, which is defined as follows:

$$E(r) = \frac{|\dot{m}_{\text{model}} - \dot{m}_{\text{exp.}}|}{\dot{m}_{\text{exp.}}} \tag{23}$$

where $\dot{m}_{\text{model}}$ is powder mass flow rate calculated by model, $\dot{m}_{\text{exp.}}$ is powder mass flow rate measured by experiment.

Otherwise, it is hard to measure the gas mass flow rate because the progress of particle pickup is so short and unsteady, there is no mass ratio of gas and solid for formula (2) to calculate the mass flow rate, so we can't do a direct accuracy comparison with current and previous model. In Ref. [21], Wang compared the experimental results with the predicted values of formula (2), so indirect comparison of two models can be carried out for error analysis. The comparison results are shown in Figs. 8 and 9, where the basic line shows the difference level between model datas and experiments, the more close to basic line for model datas, the more accurate for prediction model.

As shown in Fig. 8, the datas calculated by formula (22) are all near the basic line, otherwise, the relative errors of about 90% datas are below 15%, and the mean relative error is 6.43%, which shows

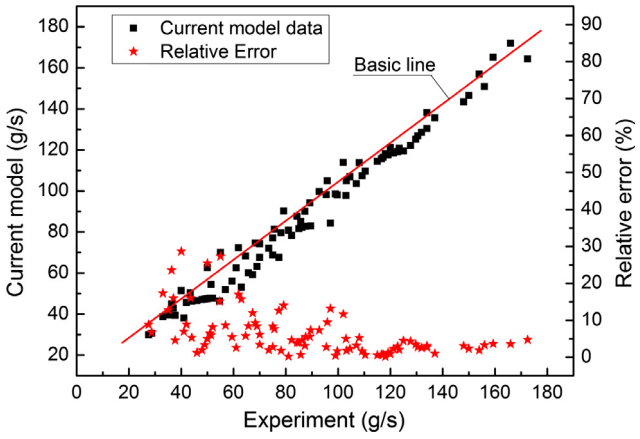


**Fig. 8.** Comparison between model (22) and experiment.

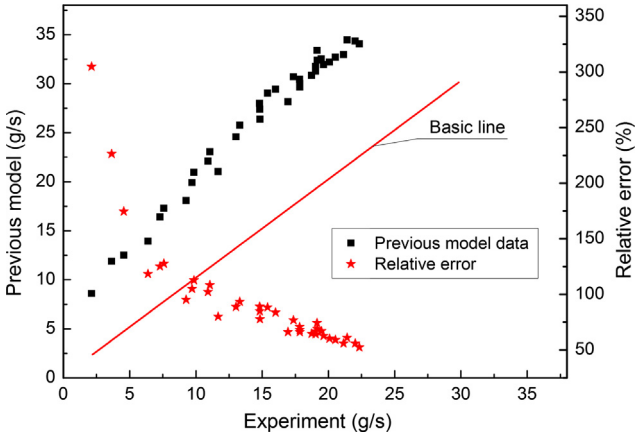


**Fig. 9.** Comparison between model (2) and experiment [21].

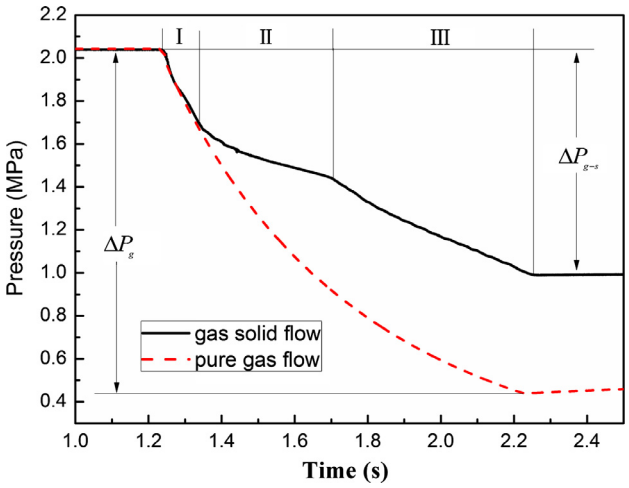


**Fig. 10.** Pressure drop comparison of pure gas flow and gas-solid flow.

the formula (22) owns good prediction accuracy. But there is a big difference for previous model (Fig. 9), all the datas are far away from basic line, and the relative errors are all greater than 50%, and worse yet, the mean relative error of formula (2) attains to 93.22%, it is unable to achieve an accurate forecast for particle mass flow rate. The trends of relative error are the same, and both of them decrease with the increase of mass flow rate.

The big prediction difference for formula (2) may be mainly attributed to the equilibrium flow model, which defines the parameters of particle velocity, particle temperature, etc. as same as the gas. Actually, there is a little possibility to form equilibrium flow by considering the influence of inter-phase coupling and particle-particle collision, etc., otherwise, particle diameter and density have a significant impact on particle mass flow rate, and there is no expression in formula (2). On the other hand, although there is a higher predicted accuracy for current model, there some uncertainty factors may affect the measurement accuracy of mass flow rate in experiment. Like vibration in operational process, humidity of gas and solid, and powder dispersion in loading process, they all will influence the initial state, flow characteristic of powder, and measurement accuracy finally.

### 4.5. Pickup progress of particle

The pressure-time curve of pure gas phase was compared with gas solid two-phase, which is shown in Fig. 10, where the initial total pressure is both 2.05 MPa. As the figure shown that the pressure-time curve of pure gas is relatively smooth, but the curve of gas-solid two-phase experiences three stages, namely, there are two turning points.

In stage I, the two curves almost overlap, which indicates that the main flow is gas in initial stage; at this time, particles have not been pickuped into tube together with gas, which shows particle entrainment has a certain delay. Afterwards, in stage II, particles flow into the tube and form gas-solid two-phase flow. The amount of gas flow-out is smaller than previous, so the rate of pressure-drop decreases and thus the curve becomes gentle. In stage III, gas-solid ratio in tube is relatively stable, so the curve becomes flat. The pressure-drop rate of stage II is smaller than that of stage III by comparing stage II and III, which indicates that the number of particles flow-out is larger than that of stage III.

The pickup progress of powder is shown in Fig. 11. Before experiment starts, there exists a cavity near the gas inlet (t = 0 s), which was formed in the progress of inflating. When the pneumatic ball valve starts to work, particles being picked up quickly and filling up the powder box (t = 0.05 s), a small amount of powder flows out (t = 0.1 s), which shows in stage I, the gas is mainly used for picking particles up, and transporting initial momentum to particles. In stage II (t = 0.2 s ~ 0.4 s), the powder level dropping

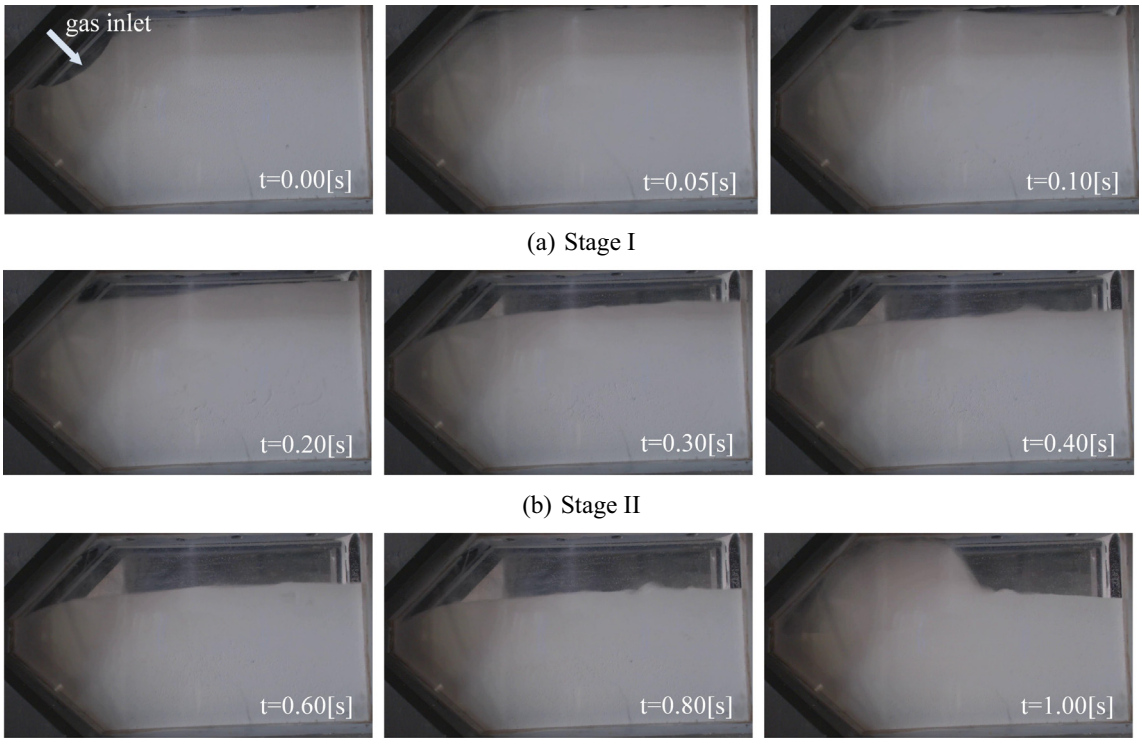


**Fig. 11.** Visualization of powder pick up.

quickly, which indicates a great deal of powder flowing out in this stage. In stage III, the decline of powder level is not obvious as stage II, so the powder outflow in stage III is smaller than that in stage II. After shutting down the pneumatic ball valve, the moving gas-solid flow meeting obstacle and then rebounding (t = 1 s).

Basically, the progresses of gas solid flow as shown in Fig. 10 and Fig. 11 are the same. The entrainment particles experience three stages in unit time: main gas flow-out stage (stage I), flow-out stage of large number of particles (stage II), and flow-out stage of small number of particles (stage III). On the other hand, the pressure-drop of pure gas phase is obviously larger than that of gas-solid two-phase by comparing the pressure drop $\Delta P_g$ with $\Delta P_{g-s}$, which indicates the gas-solid ratio in the tube has a large effect on pressure drop.

## 5. Conclusions

The incipient mass flow rate of particle in powder engine affects the determination of ignition energy directly. Experimental investigations of incipient powder mass flow rate under the influence of initial total pressure, throttling orifice area, particle sizes and powder volume fraction were carried out. Based on numerous experimental results, the corresponding relationships between those parameters were determined, and the effect laws were also presented by fitting test datas. At the same time, based on the mechanism of particle pick up, a semi-empirical model of incipient mass flow rate was established by considering numerous factors, and the coefficients of model were determined by using multivariate nonlinear regression. Through comparing the relative errors of semi-empirical model and previous model, it is found that the mean relative error of semi-empirical model is far lower than previous model, which indicates the model building is relatively reasonable, and it has good prediction accuracy.

On the other hand, in the initial entrainment process, pressure drop has three typical stages: main gas flow-out stage (stage I), flow-out stage of large number of particles (stage II), and flow-out stage of small number of particles (stage III). In stage I, the particles have not yet flown into the tube, which indicates that powder particles has a pickup delay, and this delay is very important to the ignition sequence matching research of powder engine.

## Acknowledgments

This work was supported by the National Natural Science Foundation of China (grant number 51576166).

## References

[1] H.J. Loftus, L.N. Montanino, Powder rocket feasibility evaluation, AIAA 1162 (1972).
[2] H.J. Loftus, D. Marshall, L.N. Montanino, Powder evaluation program, AD 769283 (1976).
[3] H.D. Fricke, J.W. Burr, M.G. Sobieniak, Fluidized powders – a new approach to storable missile fuels, in: 12th JANNAF Liquid Propulsion Meeting, 1970.
[4] R.A. Rhein, The Utilization of Powdered Metals as Fuels in the Atmospheres of Venus, Earth and Mars, N67-20169, 1967.
[5] R.L. Ash, W.L. Dowler, G. Varsi, Feasibility of rocket propellant on Mars, Acta Astronaut. 5 (1978) 705–724.
[6] E.Y. Shafirovish, A.A. Shiryaev, U.I. Goldshleger, Magnesium and carbon dioxide: a rocket propellant for Mars missions, J. Propuls. Power 9 (2) (1993) 197–203.
[7] E.Y. Shafirovish, A.A. Shiryaev, U.I. Goldshleger, Mars multi-sample return mission, J Brit. Inter. Soc. 48 (1995) 315–319.
[8] J.A. Linnell, T.F. Miller, A preliminary design of a magnesium fueled Martian ramjet engine, AIAA 3788 (2002).
[9] S. Goroshin, A.J. Higgins, M. Kamel, Powdered metals as fuel for hypersonic ramjets, AIAA 3919 (2001).
[10] J.P. Foote, R.J. Litchford, Powdered magnesium-carbon dioxide combustion for Mars propulsion, AIAA 4469 (2005).
[11] ONERA, RANJET, SCRAMJET and PDE – An Introduction, 2002. <http://www.orera.fr/conferences-en/ramjet-scramjet-pde/>.
[12] Zhixun Xia, Huijun Shen, Jianxin Hu, Bing Liu, Experimental investigation of powdered metals fuel ramjet, AIAA 5131 (2008).
[13] Sheng-min Zhang, Yu-xin Yang, Chun-bo Hu, Experimental investigation on thrust regulation of powdered rocket motor, J. Solid Rocket Technol. 38 (3) (2015) 347–350.
[14] Jian-zhong Liu, Jian-fei Xi, Wei-juan Yang, et al., Effect of magnesium on the burning characteristics, Acta Astronautic. 96 (2014) 89–96.
[15] Alexandre Ermoline, Deniz Yildiz, Edward L. Dreizin, Model of heterogeneous combustion of small particles, Combust. Flame 160 (2013) 2982–2989.
[16] Evgeny Rabinovich, Haim Kalman, Pickup, critical and wind threshold velocities of particles, Powder Technol. 176 (2007) 9–17.
[17] Haim Kalman, Andrei Satran, Dikla Meir, Evgeny Rabinovich, Pickup (critical) velocity of particles, Powder Technol. 160 (2005) 103–113.
[18] Devang Dasani, Charay Cyrus, Katherine Scanlon, et al., Effect of particle and fluid properties on the pickup velocity of fine particles, Powder Technol. 196 (2009) 237–240.
[19] Jie Li, J.A.M. Kuipers, Effect of pressure on gas-solid flow behavior in dense gas-fluidized beds: a discrete particle simulation study, Powder Technol. 127 (2002) 173–184.
[20] Haijun Sun, Chunbo Hu, Tian Zhang, Zhe Deng, Experimental investigation on mass flow rate measurements and feeding characteristics of powder at high pressure, Appl. Therm. Eng. 102 (2016) 30–37.
[21] Xiao-ming Wang, Qiang Li, Zong-shu Zou, et al., Experimental study on choking phenomenon of gas-powder flow, Chin. J. Process Eng. 5 (6) (2005) 591–596.
[22] F.J. Cabrejos, G.E. Klinzing, Pickup and saltation mechanisms of solid particles in horizontal pneumatic transport, Powder Technol. 79 (1994) 173–186.
[23] Evgeny Rabinovich, Haim Kalman, Incipient motion of individual particles in horizontal particle-fluid systems: a. Experimental analysis, Powder Technol. 192 (2009) 318–325.
[24] J. Hallow, Incipient rolling, sliding and suspension of particles in horizontal and inclined turbulent flow, Chem. Eng. Sci. 28 (1978) 1–12.
[25] Zhuoxiong Zeng, Turbulence Models in Dense Two-Phase Flow and its Application, China Machine Press, Beijing, 2012.